Analytica Chimica Acta 1049 (2019) 10–19

Contents lists available at ScienceDirect

Analytica Chimica Acta

journal homepage: www.elsevier.com/locate/aca

Evaluation of different competitive immunoassays for aflatoxin M_1 determination in milk samples by means of inductively coupled plasma mass spectrometry

Emma Pérez [a], Francisco M. Marco [b], Pascual Martínez-Peinado [b], Juan Mora [a], Guillermo Grindlay [a, *]

[a] Department of Analytical Chemistry, Nutrition and Food Sciences, University of Alicante, PO Box 99, 03080, Alicante, Spain
[b] Department of Biotechnology, University of Alicante, PO Box 99, 03080, Alicante, Spain

HIGHLIGHTS

- Different competitive immunoassays for AFM1 determination by ICP-MS are developed.
- Figures of merit depend on the immunoassay tracer species and the nanoparticle used.
- Developed immunoassays allow monitoring AFM1 below the maximum levels set by EU.
- Limits of detection for AFM1 in milk are improved 10-fold regarding ELISA.

GRAPHICAL ABSTRACT

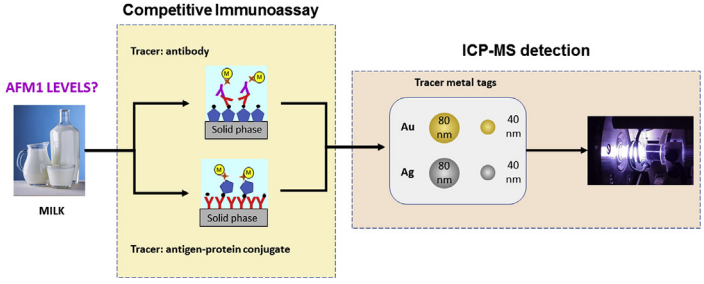

ARTICLE INFO

Article history:
Received 10 April 2018
Received in revised form
9 November 2018
Accepted 12 November 2018
Available online 13 November 2018

Keywords:
Hapten
Competitive immunoassay
Nanoparticle
Inductively coupled plasma mass spectrometry
Aflatoxin M_1

ABSTRACT

Haptens (i.e. biomolecules which molecular weight is lower than 10 kDa) determination by inductively coupled plasma mass spectrometry (ICP-MS) is usually performed by means of competitive immunoassays. In these immunoassays, analyte quantification is indirectly carried out using two different tracer species (i.e. antibodies or antigen-protein conjugates). However, the benefits (and drawbacks) derived from using a given tracer species have not been systematically investigated so far. The goal of this work is to evaluate the influence of the tracer species employed in competitive immunoassays on the analytical figures of merit for aflatoxin M_1 (AFM_1) determination in milk samples. To this end, three different strategies have been developed and evaluated, namely: (i) antibody binding inhibition assay (ABIA); (ii) capture inhibition assay (CIA); and (iii) capture bridge inhibition assay (CBIA). Experimental results show that the use of the antibody as tracer species (as in the ABIA approach) affords better analytical figures of merit for AFM_1 determination than using the antigen-protein conjugate as the tracer one (as in the CIA and CBIA strategies). The limit of detection afforded by ABIA strategy (i.e. 0.1 ng kg^{-1}) for AFM_1 determination was 1000-fold and 50-fold lower regarding the CIA and CBIA strategies, respectively. In the case of the ABIA approach, the characteristics of the metal nanoparticle label employed to detect the tracer species is critical on the analytical figures of merit. However, when the hapten-protein conjugates are used as tracer species, immunocomplex formation is severely hampered by steric effects caused by the protein moiety and, consequently, the characteristics of the metal nanoparticle label is not critical in the immunoassay performance. The different immunoassay strategies were successfully validated for AFM_1 determination in milk samples using a certified reference material of whole milk powder (ERM-BD283) according to European Conformity guidelines for analytical methods of food contaminants and

* Corresponding author.
E-mail address: guillermo.grindlay@ua.es (G. Grindlay).

https://doi.org/10.1016/j.aca.2018.11.024

mycotoxins. Compared to ELISA, the immunoassay developed for AFM_1 determination in milk samples improve limits of detection up to 10-fold.

1. Introduction

The significance of inductively coupled plasma mass spectrometry (ICP-MS) for biomolecule analysis has exponentially increased over the last years [1]. The use of ICP-MS in this field offers several attractive features regarding other established approaches: (i) high sensitivity; (ii) specificity; (iii) compound-independent detection sensitivity; (iv) multi-element capabilities; (v) robustness; and (vi) easy coupling to separation techniques. Initially, the analysis was limited to those species containing a heteroatom detectable by ICP-MS. However, analytical figures of merit were severely compromised since the heteroatoms, naturally present in biomolecules (e.g. P, S, Se, As, etc.), suffer from low sensitivity and (spectral and non-spectral) interferences due to matrix components in biological samples (e.g. carbon, chloride, etc.) [1,2]. To improve the analytical figures of merit, as well as to address with the determination of non-containing heteroatom biomolecules, different strategies have been proposed in the literature. First, the biomolecule can be derivatized through a chemical reaction with a heteroatom or an organometallic compound [3,4]. The main drawback of this approach is the low selectivity of the labelling procedure. Alternatively, the analyte of interest can be labelled by means of an immunoreaction using a heteroatom-labelled antibody [5,6]. Because of the great specificity of the antigen-antibody reaction, biomolecules can be successfully determined in complex mixtures. Heteroatoms labels used in immunoassay includes: (i) transition metals [7,8]; (ii) lanthanides [9–11]; (iii) metal nanoparticles [12–14]; and (iv) Quantum-Dots [15]. A priori, the use of metal nanoparticles is the most advantageous approach to improve analytical figures of merit (e.g. sensitivity, LoD, etc.) due to the high number of atoms present in each nanoparticle.

Non-competitive immunoassays have been traditionally employed for the analysis of high molecular weight biomolecules such as proteins, enzymes, etc. In this type of immunoassay, an antibody is usually immobilized on a solid support to capture the analyte present in the sample. Next, a different antibody, specific for another part of the biomolecule, is used to detect the analyte previously captured on the solid support (i.e. sandwich assay). The latter antibody is previously labelled with a heteroatom detectable by ICP-MS (e.g. lanthanides, Quantum-Dots, metal nanoparticles, etc.) thus enabling analyte detection. The signal registered by the ICP-MS is proportional to the analyte concentration in the sample. Dealing with haptens (i.e. biomolecules which a molecular weight is lower than 10 kDa), sandwich-based immunoassays cannot be employed since the limited surface area of this type of molecules does not allow to simultaneously accommodate two antibodies [16]. Therefore, haptens are usually determined by means of competitive-immunoassays. In this type of immunoassay, unlike non-competitive immunoassays, the quantity used of the tracer species is limited. Two different strategies have been mainly described in the literature for competitive immunoassays with ICP-MS detection so far. In the first approach, the sample is spiked with a limited amount of the antibody and the mixture is incubated on a solid phase coated with an antigen-protein conjugate. Next, a competitive reaction, for the limited number of the binding sites of the antibody, is established between the antigen bound to the solid phase and that present in the solution. The amount of the antibody retained on the solid support is inversely proportional to the antigen present in solution. To determine the antibody retained on the solid support, it should be previously labelled with a heteroatom [11]. Nevertheless, to preserve antibody activity and specificity against the antigen, it could be also detected after an immunoassay procedure using a metal-labelled secondary antibody with or without biotin-streptavidin signal amplification [11,12]. Alternatively, the competitive reaction can be also established using the antigen-protein conjugate as tracer species [14,15]. In this case, the antigen-protein conjugate is initially labelled with a heteroatom. Next, the sample is spiked with a limited amount of the labelled antigen-protein conjugate and the mixture is incubated on a solid phase coated with the antibody. Again, the amount of tracer species (antigen-protein conjugate) retained on the solid support is inversely proportional to the antigen present in the liquid phase. Up to date, both strategies have been indistinctively employed in the literature for the determination of herbicides (2,4-dichlorophenoxyacetic acid [8]), hormones (thyroxine [10], progesterone [15]), toxins (ochratoxin A [12], aflatoxin M_1 (AFM_1) [13]) and antibiotics (chloramphenicol [14]). However, the benefits (and drawbacks) derived from using either the antibody or the antigen-protein conjugate as the tracer species have not been investigated thoroughly. On the other hand, up to date there are no studies about the influence of the kind of heteroatom label employed on the analytical figures of merit of this type of immunoassays, especially for metallic nanoparticles.

The goal of this work is to perform a systematic comparison of different competitive immunoassays for hapten determination by means of ICP-MS detection. To this end, different competitive immunoassays based on the use of either antibody or antigen-protein conjugate as tracer species were investigated. Nanoparticles covering different elements (Ag/Au) and sizes (40/80 nm) were used throughout this work to evaluate their influence on the analytical figures of merit. Finally, the methods developed have been applied for the AFM_1 analysis in milk samples. Aflatoxin M_1 was selected as a model of hapten to evaluate the benefits and drawbacks of the different approaches, due to its high health risk and restrictive legal requirements.

2. Experimental

2.1. Reagents and materials

Primary rabbit polyclonal anti-aflatoxin M_1 (AFM_1) antibody (pAb) (purified IgG fraction 1 mg mL^{-1}) was obtained from Agrisera (Vännas, Sweden) whereas secondary anti-rabbit IgG (whole molecule) - Biotin antibody produced in goat (secondary Ab) (1 mg mL^{-1}) was from Sigma-Aldrich (Steinheim, Germany). According to the supplier, pAb is highly specific for AFM_1 determination with low cross-reactivity against other aflatoxins (aflatoxin B_1 2%; aflatoxin B_2, 0.4%; aflatoxin G_1 0.4% and aflatoxin G_2 0.1%).

Aflatoxin M_1 from Aspergillus flavus and AFM_1-Bovine Serum Albumin conjugate (AFM_1-BSA) were purchased from Sigma-Aldrich (Steinheim, Germany). Aflatoxins are carcinogenic compounds. So, extracts and solutions should be handled with extreme care. Gloves and other protective clothing were worn as safety

precaution during the handling of the analyte. The aflatoxin residues can be destroyed using 5% sodium hypochlorite.

Streptavidin –conjugated 40 and 80 nm Au nanoparticles and Streptavidin –conjugated 40 and 80 nm Ag nanoparticles were obtained from Cytodiagnostics (Ontario, Canada).

Sodium carbonate, sodium hydrogen carbonate, monosodium phosphate, disodium phosphate, sodium chloride, polyethylene glycol sorbitan monolaurate (Tween 20) and HPLC-grade acetonitrile were purchased from Sigma-Aldrich (Steinheim, Germany). Bovine serum albumin (BSA) was obtained from Biowest (Nuaillé, France) Iridium and rhodium 1000 mg L^{-1} stock solution was provided by Merck (Darmstadt, Germany). Thiourea, 69% w w^{-1} nitric acid and 35% w w^{-1} hydrochloric acid were purchased from Panreac (Barcelona, Spain).

Ultrapure water 18 MΩ cm from a Milli-Q system (Milli-Q water purification system, Millipore Inc., Paris, France) was used throughout the work.

Immunoaffinity columns (IACs) Afla M1 (Vicam, Watertown, MA) with a capacity of approximately 150 ng and based on monoclonal antibodies were employed for AFM_1 determination in milk samples. Amicon Ultra-4 Centrifugal Filter Units with Ultracel-10 membrane (Merck Millipore, Cork, Ireland) were used throughout the work for washing steps during the biotin labelling of the AFM_1-BSA conjugate.

For the immunoassays, F16 maxisorp polystyrene microtiter plates were purchased from Thermo- Scientific (Roskilde, Denmark) and used in all immunoassays.

2.2. Buffers and solutions

The standard stock solution of AFM_1 (5 μg mL^{-1}) was prepared by dissolving the standard AFM_1 in pure acetonitrile. Working solutions for standards or spiked milk samples were prepared by further dissolution of stock solution in incubation media or in milk, respectively. Aflatoxin M_1-BSA conjugate was dissolved in phosphate buffer saline solution for a final concentration of 500 μg mL^{-1}. Both solutions were kept at −20 °C in aliquots out of direct light and working solutions were prepared prior to each analysis. Primary rabbit polyclonal antibody was stored at 4 °C after reconstitution in 500 μL ultrapure water.

The following solutions were employed in the different immunoassays tested: (i) phosphate-buffered saline (PBS; 10 mM NaH_2PO_4, 2 mM Na_2HPO_4, 154 mM NaCl, pH 7.6); (ii) carbonate buffer solution (15 mM Na_2CO_3 and 35 mM $NaHCO_3$, pH 9.6); (iii) as plate blocking medium: 1% w V^{-1} BSA in PBS; (iv) as incubation medium: 1% w V^{-1} BSA and 0.05% V V^{-1} Tween 20 in PBS; (v) as washing medium: 0.05% V V^{-1} Tween 20 in PBS; (vi) as Au-nanoparticles digestion medium: 4% V V^{-1} nitric acid and 12% V V^{-1} hydrochloric acid; and (vii) as Ag-nanoparticles digestion medium: 2% V V^{-1} nitric acid. It is important to remark that the use of BSA in the incubation media is critical to ensure immunoassay reproducibility. Considering that the pAb was produced in rabbits by immunization with BSA haptenized with AFM_1, the pAb could react either with the AFM_1 or BSA present in the AFM_1-BSA conjugate. Moreover, bovine milk contains a significant amount of this protein (≈ 1.2% w V^{-1}). Therefore, we employed BSA as an additive in all incubation media and could consequently minimize nonspecific binding.

2.3. Immunoassay procedures

In the present work, three different competitive immunoassay strategies based on the use of either antibody or antigen-protein conjugate as tracer species were evaluated for AFM_1 determination by means of inductively coupled plasma mass spectrometry (ICP-MS) detection (Fig. 1).

2.3.1. Antibody binding inhibition assay (ABIA)

This immunoassay is based on that described in our previous work [13] in which an antibody was employed as tracer species (Fig. 1). Briefly, the competitive reaction was established between the AFM_1 present in the sample and the AFM_1-BSA conjugate, coating the solid phase, for the limited number of the binding sites of the antibody (pAb) spiked in the sample solution (Fig. 1, step 1.1–1.3). A biotinylated secondary Ab (Fig. 1, step 1.4) and streptavidin-metal nanoparticle conjugate (Fig. 1, step 1.5) were employed to detect the pAb retained on the solid phase. The incubation conditions employed are described in our previous work [13].

2.3.2. Capture inhibition assay (CIA)

This procedure is based on that previously reported by Trapiella-Alfonso et al. [17] in which a labelled antigen-protein conjugate (i.e. biotinylated AFM_1-BSA) was used as the tracer species. In this case, the competitive reaction was established between the AFM_1 present in the sample and the biotinylated AFM_1-BSA conjugate (spiked to the sample) for the limited number of the binding sites of the pAb immobilized on the solid phase. Streptavidin-metal nanoparticle conjugate was employed to detect the biotinylated AFM_1-BSA conjugate retained on the solid phase. Next CIA procedure is briefly described. First, plates were coated at room temperature with 100 μL/well of the appropriate pAb concentration in 0.05 M carbonate–bicarbonate buffer (pH 9.6). After incubation for 1 h, plates were washed three times and then blocked (200 μL/well) for 1 h at room temperature. Next, after a washing step, samples or AFM_1 standards and the appropriate biotinylated AFM_1-BSA conjugate nominal concentration were mixed (Fig. 1, step 2.1) and transferred to the solid phase (Fig. 1, step 2.2). The mixture was incubated for 1 h at room temperature and, after a washing step (Fig. 1, step 2.3), 100 μL/well of streptavidin-metal nanoparticle conjugates solution was added and incubated for 1 h at room temperature (Fig. 1, step 2.4).

2.3.3. Capture bridge inhibition assay (CBIA)

This immunoassay is based on the CIA procedure but the competitive reaction is carried out in solution. A mixture of the pAb and the biotinylated AFM_1-BSA conjugate was spiked to the sample. The competitive reaction was established between the biotinylated AFM_1-BSA conjugate and the AFM_1 present in the sample for the limited number of the binding sites of the pAb. Next, and given the bivalent nature of the antibodies, the AFM_1-pAb and the biotinylated AFM_1-BSA-pAb complexes generated were retained by the AFM_1-BSA conjugates coating the solid phase. Streptavidin-metal nanoparticle conjugates were used again to detect the biotinylated AFM_1-BSA-pAb complexes retained on the solid phase. This immunoassay strategy has never been employed for hapten analysis with to the best of author's knowledge.

The CBIA immunoassay procedure is carried out as follows. Plates were coated at room temperature with 100 μL/well of the appropriate AFM_1-BSA conjugate concentration in 0.05 M carbonate–bicarbonate buffer (pH 9.6). After incubation for 1 h, plates were washed three times and then blocked (200 μL/well) for 1 h at room temperature. Then, after a washing step, samples or AFM_1 standards, pAb and biotinylated AFM_1-BSA conjugate solutions were mixed (Fig. 1, step 3.1) and transferred to the solid phase (100μL/well) (Fig. 1, step 3.2). Next, the mixture was incubated for 1 h at room temperature. After a washing step (Fig. 1, step 3.3), 100 μL/well of streptavidin-metal nanoparticle conjugates solution was added and incubated for 1 h at room temperature (Fig. 1, step 3.4).

The biotinylated AFM_1-BSA conjugate required for the CIA and

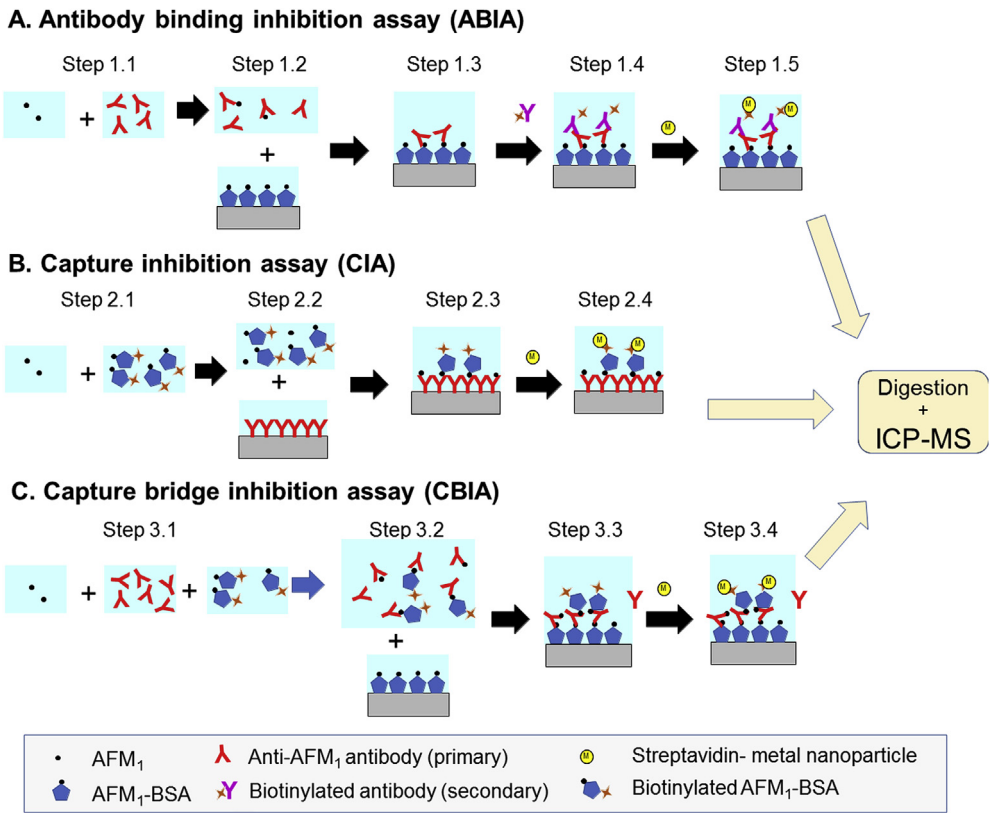

Fig. 1. Scheme of the different competitive immunoassays tested in this work.

CBIA procedures was obtained using a commercial biotin labelling kit. Briefly, 2.3 mg of succinimidyl-6-(biotinamido)hexanoate was dissolved in 500 μL of dimetylformamide and then added to a 200 μL AFM_1-BSA conjugate solution. The reaction was carried out on ice for 2 h in the dark and the excess of non-reactive biotin reagent was removed on a cutoff filter by centrifugation with PBS and recovered at a nominal concentration of 150 μg mL^{-1}. The biotinylated AFM_1-BSA conjugate solution was divided into single working aliquots and stored at −20 °C.

For all strategies, the influence of the nanoparticle chemical nature (i.e. Ag and Au) and size (i.e. 40 and 80 nm) on the analytical figures of merit was investigated. In all cases, after dissolution of the Au or Ag labelled streptavidin with 150 μL/well of the corresponding digestion acid (300 min at room temperature [12]), 50 μL/well of a 1% w V^{-1} thiourea solution containing 2.5 μg L^{-1} of the corresponding internal standard (IS) (see section 2.5) were added for a final volume of 200 μL/well and measured by ICP-MS. For the different immunoassays, Ag and Au concentration per well after the digestion procedure ranged approximately from 100 μg L^{-1} to 8000 μg L^{-1}. Standards and samples containing unknown AFM_1 amounts were run in triplicate wells and in quintuplicate wells, respectively, and the mean values were processed.

2.4. Instrumentation

Aflatoxin M_1 was indirectly quantified by means of ICP-MS using the signal of the element present in the nanoparticle ($^{107}Ag^+$ or $^{197}Au^+$). Experimental measurements were carried out on a quadrupole ICPMS model 7700x (Agilent, Santa Clara, USA). Table 1 gathers the operating conditions employed in this work.

A micronebulizer (OneNeb®, Ingeniatrics, Sevilla, Spain) coupled to a double pass quartz spray chamber (Agilent, Santa Clara, USA) was employed to introduce the sample in the plasma. Because of the limited volume of sample available in the immunoassay (200 μL), samples were introduced into a carrier stream by means of a V-451 flow injection manifold (Upchurch Scientific, Silsden, United Kingdom) equipped with a 75 μL loop valve and driven to the nebulizer by a peristaltic pump (Model Minipulse 3, Gilson, France). Carrier flow rate was set at 0.6 mL min^{-1} for high throughput analysis.

Two different carrier solutions were selected depending on the chemical nature of the nanoparticle. A mixture of 1% V V^{-1} nitric acid and 1% w V^{-1} thiourea solution was employed for $^{107}Ag^+$ measurements whereas a 1% V V^{-1} hydrochloric acid and 1% w V^{-1} thiourea mixture was employed as carrier for $^{197}Au^+$ determination. Operating in this way, no significant memory effects were registered in ICP-MS [18]. Microsoft Excel software was employed to integrate peak signals manually, given the peak-shape signal obtained with the flow injection analysis device employed.

2.5. Calibration

Internal standardization is one of the useful techniques for correction of instrument parameter fluctuation in ICP-MS. In this work, $^{103}Rh^+$ and $^{193}Ir^+$ (at final concentrations of 2.5 μg L^{-1} each one (section 2.3)) were used as an IS for $^{107}Ag^+$ and $^{197}Au^+$ measurements, respectively, due to their close atomic numbers and ionization potentials [19].

Irrespective of the immunoassay strategy employed, standard curves were obtained by plotting the metal/IS signal ratio against the logarithm of the analyte concentration because of the sigmoidal curve response of the competitive immunoassay procedure.

2.6. Samples

A certified reference material of whole milk powder (ERM-

Table 1
Operating conditions employed in ICP-MS.

Agilent 7700x ICP-MS	
Plasma forward power (W)	1550
Argon flow rate (L min^{-1}):	
Plasma	15
Auxiliary	0.9
Nebulizer	1.01
Sample introduction system	
Nebulizer	OneNeb micronebulizer®
Spray chamber	Double pass
Carrier flow rate (mL min^{-1})	0.6
Integration time (s)	0.5
Number of sweeps	100
Replicates	90
Signal nature	Area

BD283, European Commission Joint Research Centre, Geel, Belgium) containing 111 ± 18 ng kg^{-1} of AFM_1 was employed for the accuracy studies. In addition, four commercial cow milk samples obtained from retail markets were analyzed through this work. All the samples were stored at 4 °C and analyzed before their respective expiration dates.

2.7. Sample preparation

The ERM-BD283 milk powder (10.0 g) was suspended in 100 mL of warm ultrapure water (being AFM_1 final concentration of 11.1 ± 1.8 ng L^{-1}), and then processed as for milk samples.

All milk samples were pre-treated before the analysis to mitigate interferences caused by matrix components (e.g. proteins, lipids, etc.) since, otherwise, accuracy and precision would be severely compromised. To this end, two different approaches were employed through this work depending on the immunoassay employed. In the case of ABIA strategy, samples were pretreated, as described in our previous work [13], using the procedure described by Huang et al. [20] based on an extraction pretreatment into a polar solvent. On the other hand, in the case of using the antigen-protein conjugate as tracer species, milk samples were pretreated using immunocolumns following the procedure suggested by the manufacturer with some minor modifications. Briefly, a 100 mL volume of undiluted milk was centrifuged at 1614×*g* for 15 min to separate the fat and thin upper fat layer was discarded. Fifty mL of the centrifuged milk were passed through the immunoaffinity column at 1–2 drops/second by gravity. Then, the column was washed with 10 mL of water at a rate of 1–2 drops/second until air came through the column. Aflatoxin M_1 was eluted slowly from the column with 4 mL of pure acetonitrile at 1 drop/2–3 s by gravity. Two hundred μL of the sample eluate were evaporated up to dryness. The residue was reconstituted with 100 μL of PBS and then analyzed.

3. Results and discussion

Competitive immunoassays described in the literature show several differences on the experimental setup according to the tracer species monitored: i.e., the antibody [12,13] or the antigen-protein conjugate [14,15]. For the first time, immunoassays based on both approaches are compared under a similar set of experimental conditions for AFM_1 analysis.

3.1. Optimization of the immunoassay procedures

The optimization of the immunoassays tested was performed by means of checkerboard titration experiments as previously described for Enzyme Linked Immunosorbent Assay (ELISA) [21,22]. The optimum conditions were defined as the amount of reagents producing a metal-to-IS signal ratio ($^{197}Au^+/^{193}Ir^+$; $^{107}Ag^+/^{103}Rh^+$) in ICP-MS close to 80% of the maximal signal at plateau, characteristic of tracer excess conditions [21].

3.1.1. Antibody binding inhibition assay

In our previous work [13], ABIA experimental conditions were optimized using streptavidin-40 nm Au nanoparticle conjugates for AFM_1 determination in milk samples. The limit of detection (LoD) was observed to be strongly dependent on the pAb concentration. As long as the heteroatom-label allowed the accurate detection of the pAb retained on the solid phase, detection capabilities of AFM_1 could be improved decreasing the pAb concentration. In this context, high sensitive heteroatom labels are required in ICP-MS to decrease pAb concentration such as metal nanoparticles. For the first time, this works explores the influence of nanoparticle characteristics on the analytical figures of merit for a competitive immunoassay based on the use of antibodies as tracer species. To this end, nanoparticles of different chemical nature (Au and Ag) and size (80 nm and 40/80 nm, for Au and Ag, respectively) conjugated to streptavidin were investigated. For each of them, the following concentrations were optimized: (i) AFM_1-BSA conjugate; (ii) pAb; and (iii) streptavidin-metal nanoparticle conjugates. As in our previous work [13], the concentration of the secondary Ab was not optimized and the value recommended by the manufacturer was employed (0.5 μg mL^{-1}). For the sake of comparison, previous data using streptavidin-40 nm Au nanoparticle conjugates were employed [13].

First, the optimum AFM_1-BSA conjugate concentration and the optimum pAb concentration were investigated. The AFM_1-BSA conjugate concentration was modified between 0.07 and 10 μg mL^{-1} whereas the pAb concentration ranged from 0.015 to 2 μg mL^{-1}. The streptavidin-metal nanoparticle conjugates concentration was kept at 0.08 μg mL^{-1} for these experiments. The optimum AFM_1-BSA conjugate concentration was similar for all streptavidin-metal nanoparticle conjugates (i.e. 0.35 μg mL^{-1}), but significant differences were noted on the optimum pAb concentration. The optimum pAb concentration using both 80 nm Ag and Au nanoparticles was 0.015 μg mL^{-1} whereas it was 0.25 μg mL^{-1} for 40 nm Ag nanoparticles (Table S1). Interestingly, the optimum pAb concentration using 40 nm Ag nanoparticles was similar to that previously found for 40 nm Au counterparts [13]. From these findings, it could be derived that for this assay, the analytical figures of merit afforded are expected to be strongly dependent on the size of the nanoparticle employed. Fig. 2 shows the influence of the pAb concentration on the LoD (calculated as three times the standard deviation of the signal of 15 blank replicates [21,23]) using the different streptavidin-Au and Ag nanoparticle conjugates. Experimental data for 40 nm Au nanoparticles were measured following previously reported experimental conditions [13]. The only difference between the experimental set up of the metal nanoparticles investigated was the pAb concentration employed. So, it was feasible to directly evaluate the influence of the pAb concentration on the LoD. As expected, irrespective of the metal nanoparticle considered, LoD decreased when the pAb concentration was decreased. Under optimum pAb concentration, streptavidin-80 nm Au nanoparticle conjugates afforded a LoD of 0.1 ng kg^{-1}, i.e. 50-fold lower than that obtained with the 40 nm Au counterparts. Similar findings were observed for Ag nanoparticles but the LoD obtained were significantly higher than those obtained using Au nanoparticles. Thus, the LoD for 80 nm and 40 nm Ag nanoparticles were 2 and 12 ng kg^{-1}, respectively. The origin of these differences is not totally clear; since for a given nanoparticle size, optimum immunoassay conditions does not depend on the chemical nature of the

metal nanoparticle. Nevertheless, it should be considered that $^{197}Au^{+}$ sensitivity in ICP-MS is higher than that of $^{107}Ag^{+}$, mainly due to the isotopic abundance of each nuclide ($^{107}Ag^{+}$ 51.8%; $^{197}Au^{+}$ 100%). Therefore, and considering that a competitive-based immunoassay is operated, Au nanoparticles of the same size allow a better discrimination of low AFM1 levels with regard to Ag counterparts (See Fig. S1). On the other hand, it is also worth to stress that the use of Ag nanoparticles was tricky due to a build-up of Ag metallic deposits into the injector tube that could even lead to full blockage. This phenomenon was also noticed for Au nanoparticles but the metallic deposit formation was significantly lower. The influence of the streptavidin-metal nanoparticle conjugates concentration on the analytical figures of merit was also investigated. This parameter was modified between 0.02 and 0.32 μg mL^{-1}. It was observed that signals registered by the mass spectrometer increased with the streptavidin-metal nanoparticle conjugates concentration, but no changes were found in the optimum pAb and AFM$_1$-BSA conjugate concentration and, therefore, in the LoD obtained for the nanoparticles tested (Table S2). For this reason, regardless of the streptavidin-metal nanoparticle conjugate used, a concentration of 0.08 μg mL^{-1} was selected for further studies as a compromise between analytical performance and cost. These results were similar to those previously reported for 40 nm Au nanoparticles [13]; thus, pointing out that this parameter was not critical for the immunoassay performance.

Table 2 summarizes the optimum immunoassay conditions for each streptavidin-metal nanoparticle conjugate investigated. This table also includes the concentration of AFM$_1$ giving rise to a 50% inhibition (IC$_{50}$), LoD and the lower and the upper quantification limits (lLoQ and uLoQ, respectively). The lLoQ was defined as the lowest concentration that signal response has repeatability lower than 20% [24]. Similarly, the uLoQ was defined as the highest concentration that signal response has repeatability lower than 20% [24]. These analytical figures of merit were calculated from the corresponding calibration curves (Fig. 3) [21]. As expected by the changes observed on detection capabilities, IC$_{50}$, lLoQ and uLoQ depended on the streptativin-metal nanoparticle conjugate employed. For instance, IC$_{50}$, lLoQ and uLoQ experimental values for streptavidin-80 nm Au nanoparticle conjugates were 3 ng kg^{-1}, 0.3 ng kg^{-1} and 100 ng kg^{-1}, respectively. Nevertheless, the dynamic range for the different nanoparticles tested was similar.

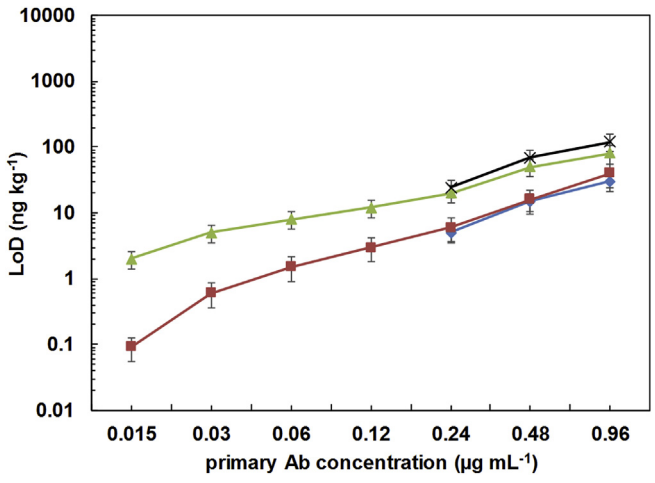

Fig. 2. Influence of the pAb concentration on the limits of detection for AFM$_1$ determination by means of ABIA procedure using different streptavidin-metal nanoparticles conjugates. (x) Ag-40 nm; (▲) Ag-80 nm; (◆) Au-40 nm; (■) Au-80 nm. Aflatoxin M$_1$-BSA conjugate concentration: 0.35 μg mL^{-1}; secondary Ab concentration: 0.5 μg mL^{-1}; streptavidin-metal nanoparticle conjugates concentration: 0.08 μg mL^{-1}. Each bar represents the mean ± t·s·n$^{-1/2}$ for three determinations (P = 95%).

3.1.2. Capture inhibition assay

Variables selected for the optimization of this immunoassay were the concentration of: (i) pAb; (ii) biotinylated AFM$_1$-BSA conjugate; and (iii) streptavidin-metal nanoparticle conjugates. Table 2 summarizes the optimum immunoassay conditions as well as some relevant analytical figures of merit (i.e. IC$_{50}$, LoD, lLoQ and uLoQ) for this immunoassay.

First, the pAb concentration and the biotinylated AFM$_1$-BSA conjugate nominal concentration were optimized. The pAb concentration ranged from 0.6 to 10 μg mL^{-1} whereas the biotinylated AFM$_1$-BSA conjugate nominal concentration was tested between 0.02 and 1.5 μg mL^{-1}. For these experiments, the streptavidin-metal nanoparticle conjugates concentration was kept constant at 0.08 μg mL^{-1}. Experimental results showed that the optimum conditions were 2.5 μg mL^{-1} for pAb and 0.05 μg mL^{-1} for biotinylated AFM$_1$-BSA conjugate (Table S3). Next, the influence of the streptavidin-metal nanoparticle conjugates concentration on the analytical figures of merit was investigated. This parameter was modified between 0.02 and 0.32 μg mL^{-1}. As it was shown for ABIA strategy, $^{107}Ag^{+}$ or $^{197}Au^{+}$ signals increased with the streptavidin-metal nanoparticles conjugate concentration but no significant changes were found in the optimum pAb and biotinylated AFM$_1$-BSA conjugate nominal concentration previously obtained as well as on the LoD (Table S4). Therefore, the streptavidin-metal nanoparticles conjugate concentration was kept at 0.08 μg mL^{-1} to minimize operative cost. Under these experimental conditions, for each of the streptavidin-metal nanoparticle conjugates (Fig. 4), a calibration curve was prepared. A LoD of 100 ng kg^{-1} was always obtained, regardless of the size and the chemical nature of the nanoparticle employed (Table 2). Though this value was similar to that previously reported for progesterone analysis [15] using an antigen-protein conjugate as tracer species, it was significantly higher than the value obtained by means of ABIA strategy. To improve the LoD, the influence of incubation time of AFM$_1$ and biotinylated AFM$_1$-BSA conjugate mixture on the microtiter plate was studied, since it could favor tracer species retention on the solid phase; thus, making feasible to use lower tracer species concentrations [13]. The incubation time was increased from 1 to 10 h, but no significant improvement on the analytical figures of merit was obtained (Table S5). From these findings, the detection capability is thought to be derived from the immunoassay procedure itself. It should be considered that, given the size of the BSA moieties (66 kDa), high steric effects are expected when biotinylated AFM$_1$-BSA conjugates are captured by the pAbs coating the microtiter plate. Obviously, steric effects are more significant as the AFM$_1$ content in the sample decreases since more biotinylated AFM$_1$-BSA conjugates are captured on the solid phase. To address this issue, some modifications were implemented in this type of immunoassay to favor the immunocomplex formation. Thus, the immunocomplexes were generated in a homogeneous phase rather than in a heterogeneous phase; minimizing steric effects and, given that the antibodies are bivalent molecules, the immunocomplexes formed were retained in a microtiter plate coated with the antigen-protein conjugate. To our best knowledge, this is the first time that this strategy is employed for hapten analysis. From now on, as mentioned above, this immunoassay will be called *capture bridge inhibition assay* (CBIA).

The optimization of CBIA was carried out likewise the CIA procedure but including the concentration of the AFM$_1$-BSA conjugates coating the microtiter plate. After some preliminary test, this concentration was observed to be not critical for the immunoassay. This reagent had just to be in excess to maximize the immunocomplex capture and, hence, this parameter was kept at 1 μg mL^{-1}.

Table 2
Optimum experimental conditions, limit of detection and dynamic range for the different immunoassay strategies.

Parameter	ABIA				CIA	CBIA
Nanoparticle	Ag		Au		Ag/Au (40/80 nm)	Ag/Au (40/80 nm)
	40 nm	80 nm	40 nm[a]	80 nm		
AFM_1-BSA conjugate (μg mL^{-1})	0.35	0.35	0.35	0.35	–	1
pAb (μg mL^{-1})	0.25	0.015	0.24	0.015	2.5	2.0
Biotinylated secondary-Ab (μg mL^{-1})	0.5				–	–
Biotinylated AFM_1-BSA conjugate (μg mL^{-1})	–				0.05	0.04
Streptavidin-metal nanoparticle conjugate (μg mL^{-1})	0.08					
IC_{50} (ng kg^{-1})	310	30	42	3	1250	78
LoD (ng kg^{-1})	12	2	5	0.1	100	5
lLoQ -uLoQ (ng kg^{-1})	30–5000	6–1250	10–2500	0.3–100	300–5000	15–1250

[a] Data taken from Ref. [13].

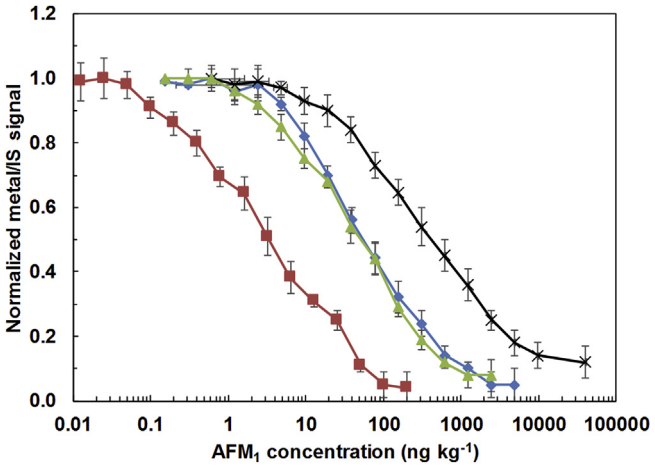

Fig. 3. Aflatoxin M_1 calibration curve using different streptavidin-metal nanoparticle conjugates for the ABIA procedure. (x) Ag-40 nm; (▲) Ag-80 nm; (◆) Au-40 nm; (■) Au-80 nm. Aflatoxin M_1-BSA conjugate concentration: 0.35 μg mL^{-1}; pAb concentration: 0.25 μg mL^{-1} (Ag-40 nm), 0.24 μg mL^{-1} (Au-40 nm), and 0.015 μg mL^{-1} (Au-80 nm and Ag-80 nm); secondary Ab concentration: 0.5 μg mL^{-1}; streptavidin-metal nanoparticle conjugates concentration: 0.08 μg mL^{-1}. Each bar represents the mean ± $t \cdot s \cdot n^{-1/2}$ for three determinations (P = 95%).

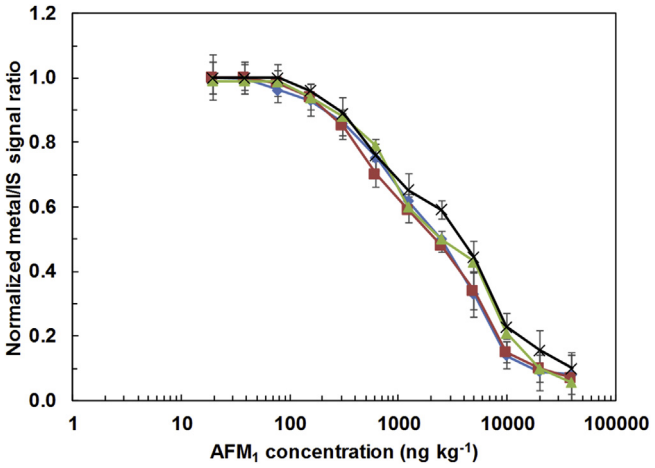

Fig. 4. Aflatoxin M_1 calibration curve using different streptavidin-metal nanoparticle conjugates for the CIA procedure. (x) Ag-40 nm; (▲) Ag-80 nm; (◆) Au-40 nm; (■) Au-80 nm. Primary antibody concentration: 2.5 μg mL^{-1}; biotinylated AFM_1-BSA conjugate: 0.05 μg mL^{-1} and streptavidin-metal nanoparticle conjugates concentration: 0.08 μg mL^{-1}. Each bar represents the mean ± $t \cdot s \cdot n^{-1/2}$ from three determinations (P = 95%).

Next, a checkerboard titration procedure was employed to optimize the biotinylated AFM_1–BSA conjugate nominal concentration and the pAb concentration. To this end, the pAb concentration was modified from 0.125 to 2 μg mL^{-1} whereas the biotinylated AFM_1–BSA conjugate nominal concentration was tested from 0.01 to 0.64 μg mL^{-1}. During this optimization, a streptavidin-metal nanoparticle conjugates concentration of 0.08 μg mL^{-1} was employed. A satisfying compromise between an optimum analytical sensitivity with a consistent readout was obtained using 2 μg mL^{-1} pAb and 0.04 μg mL^{-1} biotinylated AFM_1-BSA conjugate for all streptavidin-metal nanoparticles conjugate tested (Table S6). The influence of the streptavidin-metal nanoparticle conjugates concentration, as it was previously observed for CIA strategy, did not have a significant effect on the LoD (Table S7). Therefore, the streptavidin-metal nanoparticles conjugate concentration was again kept at 0.08 μg mL^{-1} as compromise between analytical performance and cost. Under these conditions, as it was previously noticed for the CIA procedure, LoD for AFM_1 determination was independent on the streptavidin-metal nanoparticles conjugate employed, both chemical nature and size (Fig. 5). Nevertheless, steric effects were less significant in the new approach since LoD for CBIA strategy (5 ng kg^{-1}) was improved 20-fold regarding CIA strategy (Table 2). In general, no significant differences were observed on the dynamic range for both CIA and CBIA strategies.

3.2. Comparison of the competitive immunoassays studied for AFM_1 analysis

From data gathered in the previous section, the use of the pAb as tracer species (as in the case of the ABIA procedure) seems to be more advantageous than the use of the antigen-protein conjugate as the tracer one (as in the case of CIA/CBIA strategies) for AFM_1 analysis at ultratrace levels. Immunocomplex formation in the ABIA strategy (unlike the other strategies) is not impeded by steric effects since, given the volume occupied by the BSA residues on the solid phase, pAbs have enough space to form the immunocomplexes without interacting with their neighbours (Fig. 1). In this case, the use of big diameter nanoparticles is indeed advantageous to detect low amounts of pAb retained on the solid phase. In fact, using streptavidin-80 nm Au nanoparticle conjugates, the LoD for ABIA strategy was 1000-fold and 50-fold lower regarding CIA and CBIA strategies, respectively. The LoD obtained with the ABIA method (0.1 ng kg^{-1}) was low enough to quantify AFM_1 according to the different international policies. The European Community legislation limits AFM_1 levels in milk and infant formula at 50 and 25 ng kg^{-1}, respectively; [25,26] whereas Food and Drug Administration from USA does allow AFM_1 levels up to 500 ng kg^{-1} [27]. As regards CIA and CBIA strategies, steric effects control the immunocomplex formation and, consequently, no direct advantages are

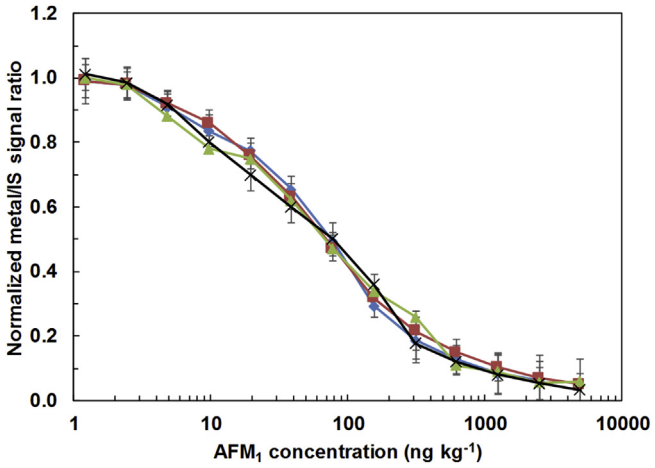

Fig. 5. Aflatoxin M_1 calibration curve using different streptavidin-metal nanoparticle conjugates for the CBIA procedure. (x) Ag-40 nm; (▲) Ag-80 nm; (◆) Au-40 nm; (■) Au-80 nm. Aflatoxin M_1-BSA conjugate: 1 μg mL^{-1}; pAb concentration: 2.0 μg mL^{-1}; biotinylated AFM_1-BSA conjugate: 0.04 μg mL^{-1} and streptavidin-metal nanoparticle conjugates concentration: 0.08 μg mL^{-1}. Each bar represents the mean ± t·s·n$^{-1/2}$ from three determinations (P = 95%).

derived from using metal nanoparticles of different chemical nature and size. Nevertheless, LoD afforded by CBIA (namely, 5 ng kg^{-1}) was still low enough to control AFM_1 levels according to international policies. Regarding the CIA method (with a LoD of 100 ng kg^{-1}), it can only be used to control the AFM_1 levels according to USA guidelines but no according to EU ones. On the other hand, an additional benefit derived from ABIA strategy was the reduction of the amount of pAb required in the immunoassay procedure by two orders of magnitude regarding CIA and CBIA strategies, thus decreasing immunoassay costs. Nevertheless, this cost reduction is counterbalanced by the need of a secondary Ab. The main benefit of using CIA and CBIA methods is the higher sample throughput since the whole immunoassay procedure takes a shorter time. Finally, no significant differences were noticed on the immunoassay dynamic range.

3.3. Method validation for AFM_1 analysis in milk

Both ABIA and CBIA methods were validated for AFM_1 analysis in milk samples according to European Conformity guidelines for analytical methods of food contaminants and mycotoxins [25,26]. Capture inhibition assay strategy was discarded due to its limited capability to control AFM_1 levels according to EU policy. Streptavidin-80 nm Au nanoparticle conjugates were used for AFM_1 determination by means of ABIA method due to its higher detection capabilities. As regards CBIA strategy, though the metal nanoparticle characteristics were not critical, 80 nm Au nanoparticles were employed for the sake of comparison. To evaluate the accuracy and precision of the methods, they were applied to the determination of AFM_1 in the ERM-BD283 milk powder reference material and recovery studies were carried out by spiking milk samples with AFM_1 standard at concentration levels over (80 ng kg^{-1}) and below (30 ng kg^{-1}) the limits established by the EU policy.

Initially, irrespective of the immunoassay procedure employed, all milk samples were analyzed after an extraction pretreatment with acetonitrile to mitigate the effects of matrix components (i.e., proteins, fats, etc.). This procedure was selected due to its simplicity and the good results afforded in our previous work using streptavidin-40 nm Au nanoparticle conjugates in the ABIA strategy [13]. However, AFM_1 recoveries were systematically higher than 100% for both ABIA and CBIA procedures using streptavidin-80 nm Au nanoparticle conjugates (Table S8). From these results, it can be derived that both types of immunoassays suffer from strong matrix effects caused by the milk components that are still present in the acetonitrile extract phase. In the case of ABIA strategy, these results could be attributed to the lower pAb concentration employed since it makes the immunoassay more sensitive to lower AFM_1 concentrations but also to matrix components. Taking into account the LoD afforded by the ABIA method, milk samples could be diluted to mitigate matrix effects without compromising analyte quantification [12]. To this end, before the extraction pretreatment, milk samples were diluted with the appropriate volume of ultrapure water. It was observed that matrix effects disappeared after a 4-fold milk dilution (Table S8). Table 3 shows the recovery values obtained for AFM_1 determination in the certified reference material and in the spiked milk samples by means of ABIA strategy after 4-fold dilution. As can be observed, good recoveries in the ranged of 93–102% were obtained. These values were within the limits established by the EU for analyte concentrations below 1 μg kg^{-1} (−40%/+20%). Taking into account the sample preparation procedure applied, LoD for AFM_1 determination by means of ABIA strategy was experimentally determined as 0.4 ng kg^{-1}. The repeatability or intra-day precision was evaluated by analyzing five replicates of each sample in the same day. The reproducibility (inter-assay precision) was determined by analyzing five replicated samples, which were spiked with the same amount of AFM_1, in five consecutive days. The intra- and inter-day precisions were expressed as the percentage relative standard deviation (RSD%). The RSDs were ranged from 2 to 10% and 5–15% for intra-day and inter-day variations respectively, which indicates good precision of the ABIA method.

As regards the CBIA strategy, the poor recoveries obtained for

Table 3
Recovery analysis of AFM_1 by ABIA and CBIA methods. Sample pretreatment: ABIA: 4-fold dilution + acetonitrile extraction; CBIA: immunocolumns.

Immuoassay	Sample	AFM_1 concentration (ng kg^{-1})		Recovery (%)[a]
		Certified/expected	Experimental[a]	
ABIA	ERM®-BD283	11.1 ± 1.8	11 ± 1	99 ± 7
	Commercial whole milk	80	81 ± 9	101 ± 8
	Commercial whole milk	30	29 ± 3	96 ± 8
	Commercial fresh milk	80	81 ± 4	101 ± 7
	Commercial fresh milk	30	31.5 ± 1.3	105 ± 4
CBIA	ERM®-BD283	11.1 ± 1.8	11.3 ± 1.2	102 ± 11
	Commercial whole milk	80	77 ± 8	95 ± 11
	Commercial whole milk	32	33 ± 4	102 ± 12
	Commercial fresh milk	80	75 ± 10	93 ± 13
	Commercial fresh milk	32	31 ± 2	97 ± 8

[a] Mean ± t·s·n$^{-1/2}$, n = 5, P = 95%.

Table 4
Comparison of different analytical methods proposed in the literature for AFM_1 determination in milk samples.

	Method	Recovery (%)	Precision (%)	LOD (ng kg^{-1})	Dynamic range (ng kg^{-1})	Reference
Immunoassays	ABIA- ICPMS	98–107	<9	0.4	1.2–1200	This work
	CBIA-ICPMS	93–102	<10	0.1	0.3–50	This work
	Direct competitive ELISA (UV-Vis detection)	90–110	<10	3	–	[28]
	Direct competitive ELISA (chemiluminiscente detection)	80–120	<10	1	2–7.5	[29]
	Indirect competitive ELISA (UV-Vis detection)	80–102	5–17	40	40–500	[30]
Liquid chromatography	Highly-sensitive time-resolved fluorescent immunochromatographic assay	80–110	5–12	0.3	0.1–200	[31]
	UHPLC-MS/MS	79	<15	0.18	50–500000	[32]
	Solid phase extraction-UPLC-MS/MS	89–120	2–9	0.3	1–300	[33]
	Liquid-liquid extraction HPLC-Fluorescence detection	73–99	2–7	50	–	[34]
	Magnetic solid phase extraction-HPLC- Fluorescence detection	91–102	5	5	15–10000	[35]
Sensors	Electrochemical immunosensor	–	–	12	15–1000	[36]
	Flow injection immunoassay	80–120	8	11	20–500	[37]

milk analysis after the extraction pretreatment could be attributed to the influence of matrix components on the biotinylated AFM_1-BSA-pAb immunocomplex formation and its retention on the microtiter plate. Unlike ABIA method, dilution could not be employed in this case since LoD would compromise AFM_1 determination according to EU policy. Consequently, dilution was discarded, and an extraction procedure based on the use of immunocolumns was selected. This approach made feasible AFM_1 analysis but at the expense of a precision decrease (Table 3). The RSD for intra-assay and inter-assay determination of AFM_1 was over 10%. Due to the extraction-preconcentration pretreatment, LoD for CBIA strategy was approximately improved 50-fold (i.e. 0.1 ng kg^{-1}) and, consequently, detection capabilities for CBIA strategy were similar to those shown by ABIA method.

Finally, both methods were applied to the analysis of commercial products (i.e. raw, pasteurized and ultra-high temperature pasteurized milk) obtained from retail markets and supermarkets. However, as expected, none of them showed detectable levels of AFM_1.

3.4. Comparison of different methodologies for AFM_1 determination

Analytical figures of merit of ABIA and CBIA procedures were compared with those previously reported in the literature for AFM_1 determination in milk (Table 4). Comparing to other competitive immunoassays and sensors, the LoD and the dynamic range are clearly improved by the immunoassays with ICP-MS detection. For instance, LoD improvement afforded by ABIA and CBIA range from 3 to 100-fold regarding ELISA procedures. Nevertheless, sample throughput is slightly reduced due to the sequential nature of the mass spectrometer. Antibody binding inhibition assay affords similar LoD than chromatographic methods but avoiding complex sample pretreatments based on solid phase extraction (such as immunocolumns) to preconcentrate and purify the AFM_1. In this regard, CBIA strategy is clearly less attractive since immunocolumns are mandatory for AFM_1 analysis. The main benefit of chromatographic methods is the feasibility to analyze several aflatoxins simultaneously.

4. Conclusions

This work demonstrates the critical role that plays the tracer species (i.e. antibody or antigen-protein conjugate) used in the competitive immunoassay for the aflatoxin M_1 determination by ICP-MS. Using the antibody as tracer species (as in the ABIA strategy), the nanoparticle-label exerts a great influence on the immunoassay experimental conditions and, consequently, on the analytical figures of merit. This type of immunoassay affords better analytical figures of merit and lower matrix effects than those based on the use of antigen-protein conjugate as tracer species (CIA and CBIA strategies). The immunocomplex formation in the latter approach is severely hampered by steric effects caused by the protein moiety in the antigen-protein conjugate. According to these results, competitive immunoassays based on the use of antibodies as tracer species seem to be more suitable for hapten analysis by means of ICP-MS detection since this strategy exploits better the detection capabilities afforded by this technique. On this regard, it is important to highlight that the use of ICP-MS detection is especially advantageous for ultra-trace determination of AFM_1 in milk samples regarding other detection approaches.

Acknowledgments

The authors would like to thank the Generalitat Valenciana (Project GV/2014/138) and the Vice-Presidency for Research and Knowledge Transfer of the University of Alicante – Spain for the financial support of this work (Project GRE12-19). E. Pérez also thanks the University of Alicante – Spain for the fellowship (UAFPU2011).

Appendix A. Supplementary data

Supplementary data to this article can be found online at https://doi.org/10.1016/j.aca.2018.11.024.

References

[1] J. Bettmer, M. Montes-Bayón, J. Ruiz Encinar, M.L. Fernández, M. Fernández de la Campa, A. Sanz-Medel, The emerging role of ICP-MS in proteomic analysis, J. Proteoms. 72 (2009) 989–1005.
[2] G. Grindlay, J. Mora, M.T.C. de Loos-Vollebregt, F. Vanhaecke, A systematic study on the influence of carbon on the behavior of hard-to-ionize elements in inductively coupled plasma-mass spectrometry, Spectrochim. Acta, Part B 86 (2013) 42–49.
[3] S. Bomke, M. Sperling, U. Karst, Organometallic derivatizing agents in bioanalysis, Anal. Bioanal. Chem. 397 (2010) 3483–3494.
[4] D. Kretschy, G. Koellensperger, S. Hann, Elemental labelling combined with liquid chromatography inductively coupled plasma mass spectrometry for quantification of biomolecules: a review, Anal. Chim. Acta 750 (2012) 98–110.
[5] C. Giesen, L. Waentig, U. Panne, N. Jakubowski, History of inductively coupled plasma mass spectrometry-based immunoassays, Spectrochim. Acta, Part B 76 (2012) 27–39.
[6] R. Liu, P. Wu, L. Yang, X. Hou, Y. Lv, Inductively coupled plasma mass spectrometry based immunoassay: a review, Mass Spectrom. 33 (2014) 373–393.
[7] T. Konz, E. Añón Alvarez, M. Montes-Bayon, A. Sanz-Medel, Antibody labeling and elemental mass spectrometry (inductively coupled plasma-mass spectrometry) using isotope dilution for highly sensitive Ferritin determination and iron-Ferritin ratio measurements, Anal. Chem. 85 (2013) 8334–8340.
[8] A.P. Deng, H.T. Liu, S.J. Jiang, H.J. Huang, C.W. Ong, Reaction cell inductively coupled plasma mass spectrometry-based immunoassay using ferrocene

tethered hydroxysuccinimide ester as label for the determination of 2,4-dichlorophenoxyacetic acid, Anal. Chim. Acta 472 (2002) 55–61.
[9] G. Schwarz, L. Mueller, S. Beck, M.W. Linscheid, DOTA based metal labels for protein quantification: a review, J. Anal. Atom. Spectrom. 29 (2014) 221–233.
[10] C. Zhang, F. Wu, X. Zhang, ICP-MS-based competitive immunoassay for the determination of total thyroxin in human serum, J. Anal. Atom. Spectrom. 17 (2002) 1304–1307.
[11] E. Pérez, K. Bierla, G. Grindlay, J. Szpunar, J. Mora, R. Lobinski, Lanthanide polymer labels for multiplexed determination of biomarkers in human serum samples by means of size exclusion chromatography-inductively coupled plasma mass spectrometry, Anal. Chim. Acta 1018 (2018) 7–15.
[12] C. Giensen, N. Jakubowski, U. Panne, M.G. Weller, Comparison of ICPMS and photometric detection of an immunoassay for the determination of ochratoxin A in wine, J. Anal. Atom. Spectrom. 25 (2010) 1567–1572.
[13] E. Pérez, P. Martínez-Peinado, F. Marco, L. Gras, J.M. Sempere, J. Mora, G. Grindlay, Determination of aflatoxin M1 in milk samples by means of an inductively coupled plasma mass spectrometry-based immunoassay, Food Chem. 230 (2017) 721–727.
[14] P. Jarujamrus R. Chawengkirttikul, J. Shiowatana, A. Siripinyanond, Towards chloramphenicol detection by inductively coupled plasma mass spectrometry (ICP-MS) linked immunoassay using gold nanoparticles (AuNPs) as element tags, J. Anal. Atom. Spectrom. 27 (2012) 884–890.
[15] A.R. Montoro Bustos, L. Trapiella-Alfonso, J.R. Encinar, J.M. Costa-Fernández, R. Pereiro, A. Sanz-Medel, Elemental and molecular detection for Quantum Dots-based immunoassays: a critical appraisal, Biosens. Bioelectron. 33 (2012) 165–171.
[16] D. Wild, The Immunoassay Handbook: Theory and Applications of Ligand Binding, ELISA and Related Techniques, fourth ed., Elsevier, Amsterdam, 2013.
[17] L. Trapiella-Alfonso, J.M. Costa-Fernández, R. Pereiro, A. Sanz-Medel, Development of a quantum dot-based fluorescent immunoassay for progesterone determination in bovine milk, Biosens. Bioelectron. 26 (2011) 4753–4759.
[18] W. Chen, P. Wee, I.D. Brindle, Elimination of the memory effects of gold, mercury and silver in inductively coupled plasma atomic emission spectroscopy, J. Anal. Atom. Spectrom. 15 (2000) 409–413.
[19] F. Vanhaecke, H. Vanhoe, R. Dams, C. Vandecasteele, The use of internal standards in ICP-MS, Talanta 39 (1992) 737–742.
[20] L.C. Huang, N. Zheng, B.Q. Zheng, F. Wen, J.B. Cheng, R.W. Han, X.M. Xu, S.L. Li, J.Q. Wang, Simultaneous determination of aflatoxin M1, ochratoxin A, zearalenone and α-zearalenol in milk by UHPLC–MS/MS, Food Chem. 146 (2014) 242–249.
[21] J.R. Crowter, The ELISA Guidebook, second ed., Humana press, New Jersey, 2001.
[22] S.J. Gee, T. Miyamoto, M.H. Goodrow, D. Buster, B.D. Hammock, Development of an enzyme-linked immunosorbent assay for the analysis of the thiocarbamate herbicide molinate, J. Agric. Food Chem. 36 (1988) 863–870.
[23] W. Jiang, Z. Wang, G. Nolke, J. Zhang, L. Niu, J. Shen, Simultaneous determination of aflatoxin B1 and aflatoxin M1 in food matrices by enzyme-linked immunosorbent assay, Food Anal. Meth. 6 (2013) 767–774.
[24] Guidance for Industry, Bioanalytical Method Validation, US Department of Health and Human Services, Food and Drug Administration Centre for Drug Evaluation and Research (CDER), Centre for Veterinary Medicine (CVM), May 2001.
[25] EC, Commission Regulation (EC) No. 1881/2006 of 19 December 2006 setting maximum levels for certain contaminants in foodstuffs, Offic. J. Eur. Union L 364 (2006) 5–24.
[26] EC, Commission regulation, regards aflatoxins and ochratoxin a in foods for infants and young children, Offic. J. Eur. Union L 106 (2004) 5–24.
[27] FDA, Sec, 527.400 Whole Milk, Low Fat Milk, Skim Milk – Aflatoxin M1 (CPG7106.10), FDA/ORA Compliancy Guides, 2005.
[28] D. Guan, P. Li, W. Zhang, D. Zhang, J. Jiang, An ultra-sensitive monoclonal antibody-based competitive enzyme immunoassay for aflatoxin M1 in milk and infant milk products, Food Chem. 125 (2011) 1359–1364.
[29] M.M. Vdovenko, C.C. Lu, F.Y. Yu, I.Y. Sakharov, Development of ultrasensitive direct chemiluminescent enzyme immunoassay for determination of aflatoxin M1 in milk, Food Chem. 158 (2014) 310–314.
[30] S.C. Pei, Y.Y. Zhang, S.A. Eremin, W.J. Lee, Detection of aflatoxin M1 in milk products from China by ELISA using monoclonal antibodies, Food Contr. 20 (2009) 1080–1085.
[31] X. Tang, Z. Zhang, P. Li, Q. Zhang, J. Jiang, D. Wang, J. Lei, Sample-pretreatment-free based high sensitive determination of aflatoxin M1 in raw milk using a time-resolved fluorescent competitive immunochromatographic assay, RSC Adv. 5 (2015) 558–564.
[32] W.L. Chen, T.F. Hsu, C.Y. Chen, Measurement of aflatoxin M1 in milk by utra-high-performance liquid chromatography/tandem mass spectrometry, J. AOAC Int. 94 (2011) 872–877.
[33] X. Wang, P. Li, Rapid screening of mycotoxins in liquid milk and milk powder by automated size-exclusion SPE-UPLC–MS/MS and quantification of matrix effects over the whole chromatographic run, Food Chem. 173 (2015) 897–904.
[34] P. Diniz Andrade, J. Laine Gomez da Silva, E. Dutra Caldas, Simultaneous analysis of aflatoxins B1, B2, G1, G2, M1 and ochratoxin A in breast milk by high-performance liquid chromatography/fluorescence after liquid-liquid extraction with low temperature purification (LLE-LTP), J. Chromatogr. A 1304 (2013) 61–68.
[35] M. Hashemi, Z. Taherimaslak, Determination of aflatoxin M1 in liquid milk using high performance liquid chromatography with fluorescence detection after magnetic solid phase extraction, RSC Adv. 4 (2014) 33497–33506.
[36] A. Vig, X. Muñoz-Berbel, A. Radoi, M. Cortina-Puig, J.L. Marty, Characterization of the gold-catalyzed deposition of silver on graphite screen-printed electrodes and their application to the development of impedimetric immunosensors, Talanta 80 (2009) 942–946.
[37] M. Badea, L. Micheli, M.C. Messia, T. Candigliota, E. Marconi, T. Mottram, M. Velasco-Garcia, D. Moscone, G. Palleschi, Aflatoxin M1 determination in raw milk using a flow-injection immunoassay system, Anal. Chim. Acta 520 (2004) 141–148.